Chemical Engineering Journal 162 (2010) 266–272

Contents lists available at ScienceDirect

Chemical Engineering Journal

journal homepage: www.elsevier.com/locate/cej

Cr(VI) reduction by activated carbon and non-living macrophytes roots as assessed by Kβ spectroscopy

Aparecido N. Módenes[a], Fernando R. Espinoza-Quiñones[a,*], Soraya M. Palácio[a],
Alexander D. Kroumov[b,1], Guillermo Stutz[c], German Tirao[c], Adriana S. Camera[a]

[a] Parana West State University (UNIOESTE), Department of Chemical Engineering, Post Graduate Program, rua da Faculdade 645, 85903-000 Toledo, Paraná, Brazil
[b] University of Kentucky, Center of Applied Energy Research and Biosystem Agricultural Engineering, 212 C.E. Barnhart Building, Lexington, KY 40546-0276, United States
[c] Universidad Nacional de Córdoba, Facultad de Matemática, Astronomía y Física, Medina Allende y Haya de la Torre, 5000 Córdoba, Argentina

ARTICLE INFO

Article history:
Received 4 April 2010
Received in revised form 20 May 2010
Accepted 21 May 2010

Keywords:
Cr(VI) reduction
Adsorption
High-resolution Kβ spectroscopy

ABSTRACT

In this work, the behavior of cationic-exchange resin, activated carbon, and non-living aquatic macrophytes biomasses on the Cr(VI) and Cr(III) uptake and Cr(VI) reduction was investigated. The high-resolution X-ray fluorescence (HR-XRF) technique was used to study the adsorption process, as well as to study Cr(VI) reduction and removal from metal solutions. Batch Cr ions sorption experiments at pH 3.5 were carried out in order to speciate 3d-transition metal onto the surface of these types of adsorbents by a Kβ spectra analysis. Cr-Kβ satellite lines have been characterized for all Kβ spectra of Cr ions onto treated samples and reference material. Based on their energy position and intensity of Cr-Kβ satellite lines as well as their related to reference material shift energy, activated carbon and non-living aquatic macrophytes roots were found to act mainly as good adsorbents, first reducing Cr(VI) to Cr(III) and then followed by a Cr(III) adsorption. Although cationic-exchange resin was treated with Cr(VI) solution, no evidence of any Cr-Kβ spectral satellite lines was shown in it, suggesting that Cr(VI) was not removed in a cationic-exchange process. Evidence of reduction of hexavalent chromium by adsorbent materials was assessed by Kβ spectral lines analysis.

1. Introduction

Environmental pollution by the introduction of heavy metals into bodies of water is of growing concern because of health risks on living organisms and humans. Hexavalent and trivalent chromium are released into the environment from a number of different industrial activities such as iron and steel manufactory, tannery, chromium plating and other anthropogenic sources [1]. Usually, conventional treatment methods are applied in industries for Cr(VI) removal by its reduction to Cr(III) with reducing agents, followed by a precipitation of a hydroxide form of Cr(III).

Many treatment technologies have been proposed to solve this problem and replace the high cost, conventional treatment process. Among these technologies, adsorption that is one most frequently used method has gained increased creditability during the last decades [2,3]. There are many types of adsorbents that have been studied for the metal ions adsorption from aqueous solutions, such as activated carbon [4], sawdust [5,6], chitosan [7], chelating resins [8,9], clay mineral [10,11], non-living aquatic plants [12–14] and wetland plants [15–19].

In order to gain information about these chemically important systems, X-ray emission spectroscopy could be an adequate tool in the study of the 3d metal removal process such as chromium ions in different kind of materials. A recent review of Kα and Kβ spectroscopy has shown the chemical sensitivity of the fluorescence transitions that could be applied to study 3d metal transition complexes [20]. The Kα lines are the strongest fluorescence transitions that are the contribution of X-ray transitions from 2p to 1s electronic state. The X-ray fluorescence transitions denoted as Kβ satellite lines are weaker than Kα ones. These latter X-ray lines are fluorescence transitions from orbitals higher than the metal 3p shell that are often dominated by the oxidation state and chemical environment.

When a synchrotron radiation-based X-ray emission spectroscopy is used to speciate 3d-transition metal, the metal Kβ spectra could be enhanced in order to measure the Kβ transition energies and intensities. In addition, in order to be able to separate spectral features within the Kβ group and detect changes of the spectral shape due to the chemical environment, it is necessary to achieve a resolving power of order $E/\Delta E > 5000$, which currently can only be obtained with a spectrometer based on perfect-crystal Bragg optics [20].

---

* Corresponding author. Tel.: +55 45 3379 7092; fax: +55 45 3379.7002.
E-mail addresses: f.espinoza@terra.com.br, espinoza@unioeste.br
(F.R. Espinoza-Quiñones).

[1] b-former address.

1385-8947/$ – see front matter © 2010 Elsevier B.V. All rights reserved.
doi:10.1016/j.cej.2010.05.045

Nomenclature

E_{abs}	absorption edge energy (eV)
E	spectral line energy (eV)
h_0	upper base-line position
h	step high
x, x_0	analyzer positions
w	width of the absorption edge (eV)
Kα	X-ray transitions from 2p to 1s electronic state
K$\beta_{1,3}$	X-ray transitions from 3p to 1s electronic state
K$\beta_{2,5}$	X-ray transitions from molecular orbitals to 1s electronic state
Kβ''	X-ray transitions from ligands s-electrons to 1s electronic state
θ_{B}	Bragg angle

In this work, as an essential aid to understanding the Cr(VI) reduction and Cr ions sorption in Amberlite IR 120 cationic-exchange resin, activated carbon, and non-living aquatic macrophytes biomasses, a combination of the high-resolution X-ray fluorescence (HR-XRF) technique and a high flux, 6.1-keV X-ray monochromatic beam was used to enhance the spectral satellite lines that are chemically dependent. A hypothesis was proposed for Cr(VI) reduction as a function of an adsorption process, and it was proved by Kβ spectroscopy results.

2. Materials and methods

2.1. Adsorbents and chemicals

For the study of hexavalent chromium reduction during the removal process, three kinds of materials were tested: a cationic-exchange resin, an activated carbon, and two non-living aquatic macrophytes. The Amberlite® IR 120 in the Na$^+$ form (CAS # 9002-23-7) was used as a strong acidic cation-exchange resin. It is a gel type strongly acidic exchange resin with the sulfonic groups (SO_3–Na) on styrene–divinylbenzene copolymeric backbone, produced by Rohm and Hass Company. It has the advantages of high exchange rate, high capacity, and strong mechanic strength. The granular activated carbon, prepared in thermal carbonization of animal bones, was used as a common adsorbent. Samples of biomass of aquatic macrophytes *Pistia stratiotes* and *Salvinia auriculata* were dried at a 30 °C oven and mechanically ground and further were used as an alternative biosorbent.

The chemicals used were of analytical-reagent grade. Deionized waters were also used as dilution media. Several stock solutions of Cr(III) and Cr(VI) in deionized waters were prepared, with 8.0 mequiv. L^{-1}, from their water-soluble metallic salt ($Cr(NO_3)_3{\cdot}9H_2O$ and CrO_3, Merck pro analysis) and stored in 1-L volumetric flasks for posterior metal adsorption experiments. Solutions of NaOH (1 M) and HCl (1 M) were also used as a pH adjustment. Based on a chromium standard solution (1.0 g L^{-1} for AAS, Merck), different diluted-Cr concentrations ranging from 0.1 to 15 mg Cr L^{-1} were also prepared and used to obtain the calibrate curve for atomic absorption spectrometer (AAS). At each metal uptake experiment, the mean Cr concentration in the 0.45-μm membrane filtrated liquid phase was determined, using a previously calibrated AAS (AA 932-GBC, Analitica).

2.2. Chemical species of Cr

The EDTA-based-colorimetric method [21,22] was applied to the Cr(III) determination in two types of Cr solutions. An amount of 5-g EDTA was weighed and added to a 125-mL beaker, containing 50 mL Cr solution. The beakers were heated up to boil the solution with occasional swirling for 40 min [23]. The solutions were cooled and then quantitatively transferred with deionized water rinses to individual volumetric flasks. The absorbance of Cr(III) in each solution was measured using a UV–vis spectrophotometer (Shimadzu, model UV – 1601 PC) at 540-nm wavelength. All the extractions that involved EDTA agent were carried out at pH 3.0. Then the calibration curve was drawn using the appropriate Cr(III) standards. The total chromium concentration in liquid phase was determined from triplicate samples, using a previously calibrated AAS (AA 932-GBC, Analitica). All measurements were made at the 357.9 nm Cr wavelength, using a Cr hollow-cathode lamp. The total amount of Cr(VI) was determined in each solution by the subtraction of Cr(III) from the total chromium in the Cr(VI) solution.

2.3. Kinetic test

In order to perform kinetic experiments, 25 mg of Amberlite IR-120 cationic-exchange resin beads, activated carbon, and dry macrophytes root powder samples were put into contact with 50 mL of solution, at 3.0 initial pH, containing approximately 8.0 mequiv. L^{-1} of Cr(III) and Cr(VI). The mixtures have been stirred on a shaker at 30 °C constant controlled temperature. The solution pH measurements were carried out during the sorption experiments and the pH adjustment to 3 was made as required. The adsorption experimental times were set up with contact time ranging from 0 to 48 h, in order to determine the equilibrium time. In this way, a whole sample was taken at each setting time and the liquid phase was separated from the adsorbent using a vacuum filtration system. Afterwards, the initial and final chromium concentrations in each liquid phase were determined by AAS.

2.4. Batch Cr ions uptake experiments

For Cr(VI) uptake experiments, 25 mg of activated carbon, dry macrophytes root powder, or cationic-exchange resin was added to a 50-mL Cr(VI) solution on approximately 8.0 mequiv. L^{-1} (70 mg L^{-1}) at 3.0 initial pH. The solution pH monitoring was carried out during all experiments and the pH adjustment to 3 was made as required. The mixtures were agitated on a shaker at 30 °C constant controlled temperature for 8 h. Further, the samples liquid phase was separated from the adsorbent using a vacuum filtration system. The initial and final chromium concentrations in each liquid phase were determined by AAS. Cr(VI) uptake experiments were performed in 12 replicates. The same procedure was carried out to study the Cr(III) uptake in activated carbon, dry macrophytes root powder, and cationic-exchange resin by applying 8.0 mequiv. Cr(III) L^{-1} (140 mg L^{-1}) solutions.

2.5. Sample preparation for Kβ spectra analysis

For Kβ spectra analysis, 100 mg of each kind of Cr treated sample was pressed into pellets of a 5-mm diameter, using a 2-ton press. In order to calibrate the Cr-Kβ spectra, a pure metallic chromium foil was also used as reference material. Other pellets made from Cr_2O_3, CrO_2, and CrO_3 powder were also prepared under similar conditions, as trivalent, tetravalent, and hexavalent chromium references, respectively.

3. Results and discussion

3.1. Speciation of chromium

From a qualitative analysis point of view, the results from the EDTA colorimetric method-based Cr(III) chemical extraction from Cr(VI) solution have shown that there is no presence of Cr(III)

Table 1
Parameters of spectral lines for metallic chromium and chromium compounds.

Reference material	Oxidation state	$K\beta_{1,3}$ energy[a] (eV)	$K\beta_{2,5}$ energy[a] (eV)	$K\beta''$ energy[a] (eV)
Cr	0	5946.71 ± 0.04[b]	5988.19 ± 0.09	
Cr_2O_3	III	5947.81 ± 0.05	5985.43 ± 0.05	5969.73 ± 0.23
CrO_4	IV	5947.39 ± 0.06	5986.64 ± 0.06	5970.66 ± 0.15
CrO_3	VI	5945.67 ± 0.03	5989.90 ± 0.08	5973.37 ± 0.08

[a] Centroid of Gaussian peak.

[b] Cr-$K\beta_{1,3}$ according to the tabulated values by Bearden (1967) [24].

species during the course of the adsorption experiments (data not shown), suggesting that the reduction of Cr(VI) to Cr(III) in pH 3.0 was not found [23].

In addition, the analysis of the intensity of the area of Cr-$K\beta_{2,5}$ satellite line in all Kβ spectra (data shown in Section 3.6), showed a great amount of Cr(III) removed from the Cr(III) solution at pH 3 using the Amberlite IR-120 cationic-exchange resin. From the Cr(VI) uptake tests using cationic resin and mixtures of cationic resin and dried aquatic plant biomass (*S. auriculata* or *P. stratiotes*), which were added to Cr(VI) solution, keeping at pH 3, it was observed that there was no evidence of a characteristic Cr-$K\beta_{2,5}$ peak associated with Cr(III) or Cr(VI) to be found in resin samples. However, Cr-$K\beta_{2,5}$ peaks associated with Cr(III) were only observed for aquatic plant samples. Based on these preliminary results, we can be conclude that there is no evidence for Cr(VI) to Cr(III) reduction in the solution, as also suggested by the results from EDTA colorimetric method.

3.2. Kinetic test

The uptake of chromium ions has increased sharply at short contact and slowed gradually as equilibrium was approached. For *P. stratiotes*, *S. auriculata*, and cationic-exchange resin the equilibrium time was around 2 h, with Cr(III) removal rates of 53.7, 64.6, and 99.9%, respectively, while for activated carbon it was 6 h and 68.3% removal rate. In Cr(VI) uptake experiments, a 6-h equilibrium time was achieved to the *P. stratiotes*, *S. auriculata*, and activated carbon, with removal rates of 41.5, 34.8, and 24.9%, respectively. Under the same experimental conditions for cationic-exchange resin, during the first 2 h 7.1% reduction of Cr(VI) initial concentration-relative-to was observed.

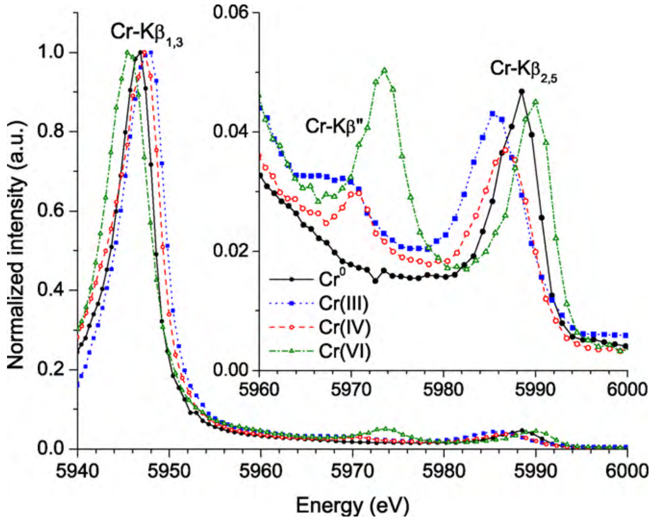

Fig. 1. Cr-Kβ spectra for metallic Cr and Cr compounds (Cr_2O_3, CrO_2, and CrO_3). Black (solid), blue (dot), red (dash), and green (dash-dot) lines correspond to Cr^0, Cr(III), Cr(IV), and Cr(VI), respectively.

3.3. Kβ satellite lines in reference materials and samples

The Cr-Kβ emission spectrum of each sample was measured in two energy regions. The first one (5940–5960 eV) comprised the main $K\beta_{1,3}$ peak and the second one (5960–6020 eV) comprised the $K\beta_{2,5}$ and $K\beta''$ satellite lines, which provide information about the oxidation state and the chemical ligand, respectively. Typical measuring time of a complete Cr-Kβ scan for reference samples (Cr metal foil, Cr_2O_3, CrO_4, and CrO_3 pellets) was about 5–20 min, whereas for an activated carbon sample it was about 2 h. About 2×10^4 counts were accumulated in a single measuring point at the maximum of the $K\beta_{2,5}$ line. For each chromium ions treated material, the Kβ emission spectrum was measured. Typical measuring time of a whole Cr-Kβ scan for a sample was about 2 h. About 200 counts per second were accumulated in a single measuring point at the maximum of the $K\beta_{2,5}$ line. The procedure was applied for all samples.

The normalized-to-monitor Cr-Kβ spectra were performed due to the systematically decreasing of X-ray beam flux during the oper-

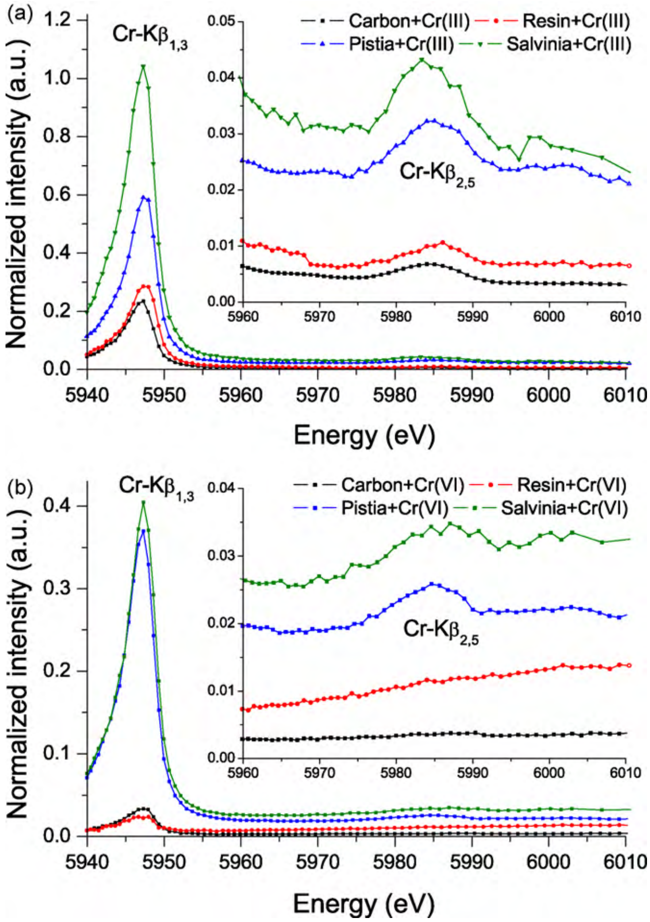

Fig. 2. Cr-Kβ spectra of carbon, resin, *Pistia* and *Salvinia* samples after the adsorption processes in (a) trivalent and (b) hexavalent Cr solutions.

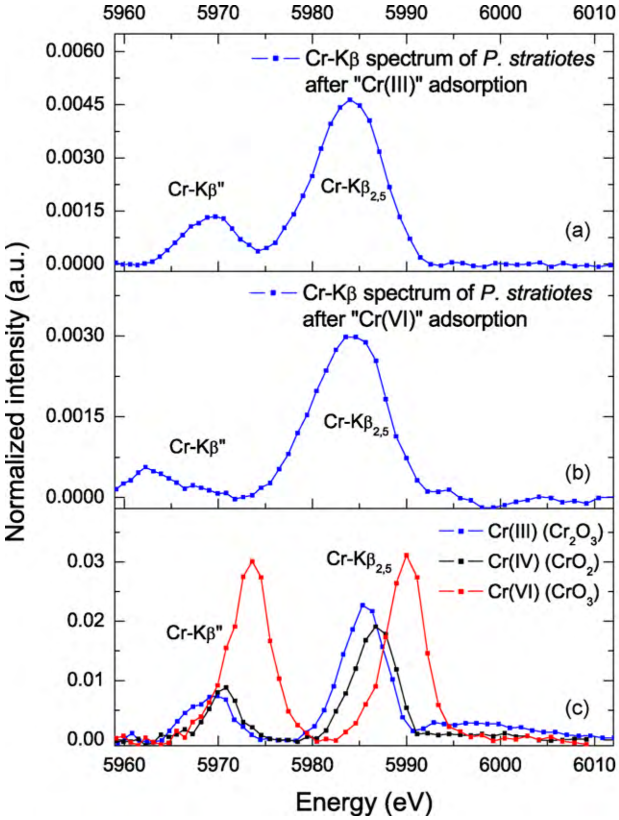

Fig. 3. Comparison between the partial Kβ spectra in the energy region of $K\beta_{2,5}$ of *Pistia stratiotes* samples after the Cr adsorption processes of (a) trivalent, (b) hexavalent Cr solutions, and (c) Cr-Kβ spectra of reference materials.

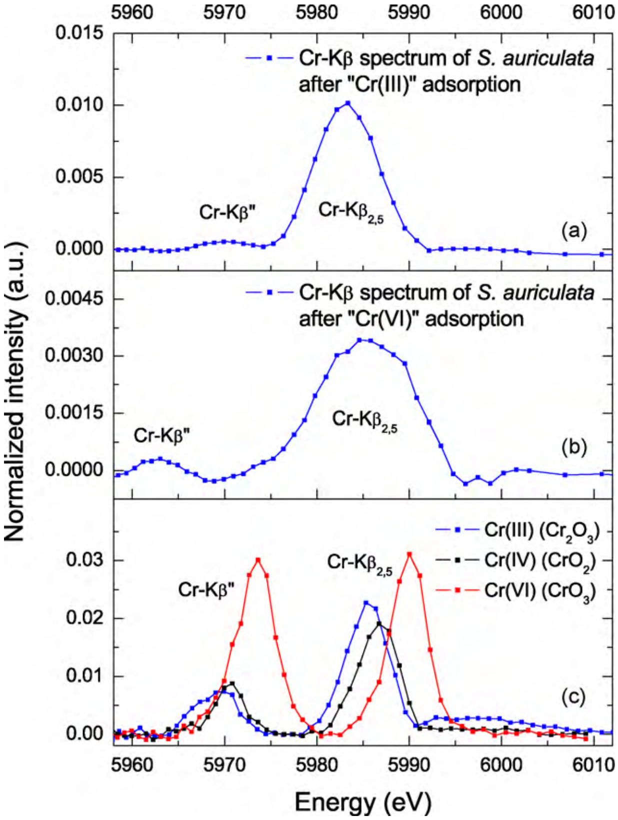

Fig. 4. Comparison between the partial Kβ spectra in the energy region of $K\beta_{2,5}$ of *Salvinia auriculata* samples after the Cr adsorption processes of (a) trivalent, (b) hexavalent Cr solutions, and (c) Cr-Kβ spectra of reference materials.

ation of the 1.37 GeV storage ring of the LNLS. A photon energy scale of Cr-Kβ spectra was obtained using the well-known energy of Cr-$K\beta_{1,3}$ line (5946.71 eV) [24] and its corresponding analyzer position in chromium metal spectrum, according to Eq. (1):

$$E\ \ (\mathrm{eV}) = 5946.71\ \ \mathrm{eV}\frac{\sin[\theta_B(\mathrm{Cr}^0)]}{\sin[(x_0 - x)(8.85/3600) + \theta_B(\mathrm{Cr}^0)]} \tag{1}$$

where, x is the analyzer position, x_0 is the analyzer position on $K\beta_{1,3}$ line belonging to Cr^0 (5946.71 eV), and θ_B is the Bragg angle (85.824°) on the same spectral line.

3.4. Chemical shift and environmental effects on Kβ lines

Typical monitor-normalized Cr-Kβ spectra of chromium reference materials are shown in Fig. 1. At 5940–5960 eV region, main spectral line ($K\beta_{1,3}$) of three Cr oxidation states was observed and its energy was measured by multi-peak fitting using Gaussian-type functions, showing that they are rather shifted with respect to that of Cr^0 due to a slight dependence on the metal oxidation state, as summarized in Table 1. This kind of spectral line is governed by the contribution of unresolved X-ray transitions from the $3p_{1/2}$ and $3p_{3/2}$ to the 1s electronic state. In higher energy region, the Cr-$K\beta_{2,5}$ and Cr-$K\beta''$ lines are displayed in the inset of Fig. 1. The Cr-$K\beta_{2,5}$ line corresponds to the unresolved multiplet transitions from molecular orbitals (Cr 3d electrons) to the Cr 1s core level, being the transition energies strongly dependent on the oxidation state [20,25,26]. However, the Cr-$K\beta''$ line is originated by the unresolved multiplet transitions from ligands s-electrons (molecular orbital) to Cr 1s core level, which can also be used as a fingerprint for the presence of chemical bonds in samples [25,27].

3.5. Enhancements of Kβ satellite lines

The monitor-normalized Cr-Kβ spectra of chromium ions uptake by different materials (*P. stratiotes*, *S. auriculata*, activated carbon, and cationic-exchange resin) are shown in Fig. 2. In addition, the Cr-$K\beta_{2,5}$ and Cr-$K\beta''$ lines are displayed in the inset of Fig. 2. In these spectra, the Kβ satellite lines (Cr-$K\beta_{2,5}$ and Cr-$K\beta''$) are superimposed over a prominent background, which consists of a matrix contribution due to the inelastic X-ray scattering from the bulk of the material, a step-like component associated with the Cr-K absorption edge (around 5991 eV) and Cr-$K\beta_{1,3}$ peak contribution.

In order to estimate the matrix background, a Gaussian-type curve was fitted to the high-energy region (5970–6040 eV) of material bulk spectrum. The matrix contribution was then subtracted from the monitor-normalized Cr-Kβ spectra [23]. This latter procedure was not applied only for chromium reference materials. Afterward, the step-like background was estimated by Eq. (2) and then subtracted from the Cr-Kβ spectra. A Lorentzian-type function was used to fit the Cr-$K\beta_{1,3}$ peak contribution and then subtracted from the Cr-Kβ spectra in order to enhance the Cr-$K\beta''$ peak.

$$f(E) = h_0 - \frac{h}{1 + \exp\left[\frac{E_{\mathrm{abs}} - E}{w}\right]} \tag{2}$$

where, E_{abs} is the Cr-K absorption edge energy, w is the experimental width of the Cr-K absorption edge, and the fitting parameters h_0 and h stand for the upper base-line and step high, respectively.

The energies of Cr-$K\beta_{2,5}$ peak of reference materials (Table 1) were determined from a Gaussian-type function fit to the background-subtracted Cr-Kβ spectra. In Table 1, the chemical shift and environmental effects on the peak intensity and peak energy are evident, confirmed by the shifted-to-metallic chromium peak

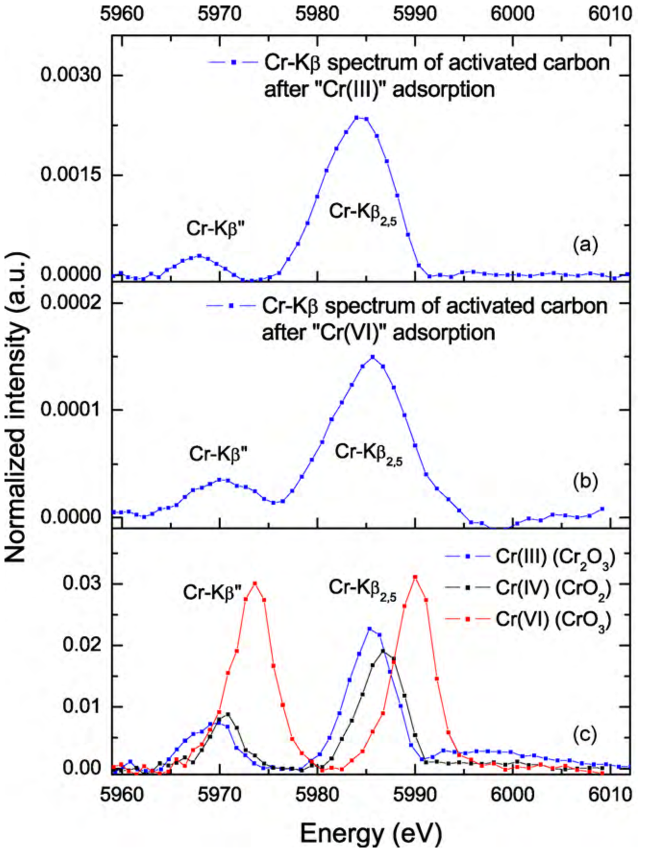

Fig. 5. Comparison between the partial Kβ spectra in the energy region of Kβ$_{2,5}$ of activated carbon samples after the Cr adsorption processes of (a) trivalent, (b) hexavalent Cr solutions, and (c) Cr-Kβ spectra of reference materials.

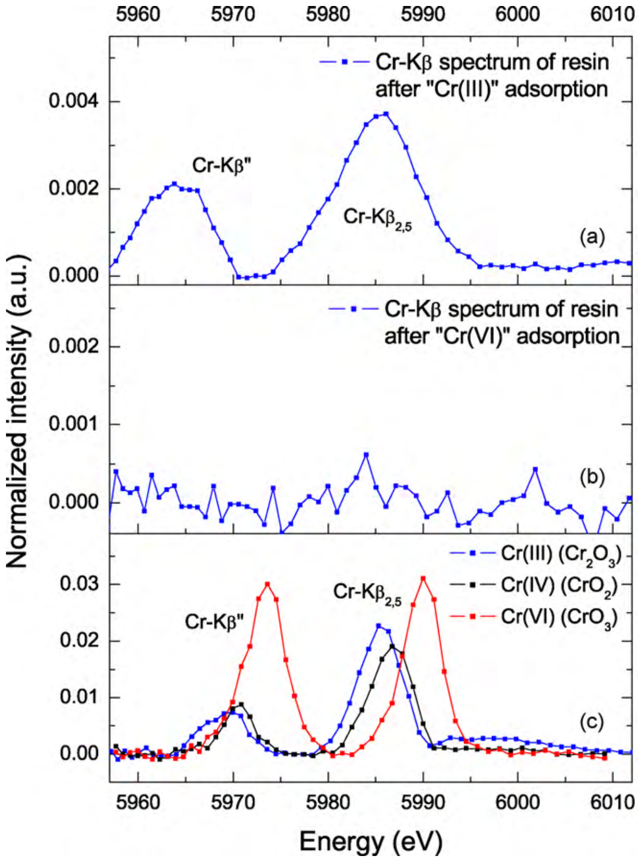

Fig. 6. Comparison between the partial Kβ spectra in the energy region of Kβ$_{2,5}$ of cationic resin samples after the Cr adsorption processes of (a) trivalent, (b) hexavalent Cr solutions, and (c) Cr-Kβ spectra of reference materials.

energy for the three-oxidation states of chromium. Apart from the slight line energy of these Cr oxidation states, the Cr-Kβ″ line intensity is stronger for chromium in hexavalent form than the other ones. Based on both Cr-Kβ$_{2,5}$ and Cr-Kβ″ spectral lines, the oxidation state of chromium and chemical ligands in different materials could be investigated. In addition, with the help of Kβ spectroscopy a new insight of Cr(VI) reduction to less toxic form was found. This gave us a basis for proposing the following hypothesis: the Cr(VI) to Cr(III) reduction is mediated by an adsorption process onto the adsorbent surface, regardless of the type of the chosen biosorbent.

3.6. *Experimental evidence of Cr(VI) reduction*

The background-subtracted Cr-Kβ spectra that are restricted to the satellite line energy region of *P. stratiotes*, *S. auriculata*, activated carbon, and cationic-exchange resin after adsorption process of chromium ions are shown in Figs. 3–6, respectively. In addition, the Cr-Kβ spectra of Cr(III), Cr(IV), and Cr(VI) reference materials are also shown where the Cr-Kβ$_{2,5}$ peak energy of Cr(III) was found to be the lowest one. At all Cr-Kβ spectra, it was confirmed that the Cr-Kβ″ line energies (transitions from molecular orbitals) are strongly dependent on the oxidation state and chemical ligand. The characteristics of both the energy and the intensity of satellite lines could be used as a fingerprint of Cr(VI) or Cr(III) in Cr treated materials.

In Cr-Kβ spectra of all materials (*P. stratiotes*, *S. auriculata*, activated carbon, and cationic-exchange resin) after Cr(III) adsorption processes (see Figs. 3a, 4a, 5a, and 6a), the peak energies of Cr-Kβ$_{1,3}$ are almost the same value when compared but there is a very slight shift for the Cr(III) reference material due to the chemical ligand effect (Fig. 7a). This effect is more evident in the energy of Cr-Kβ$_{2,5}$ and Cr-Kβ″ satellite lines (see Table 2). There is experimental evidence [23,25] that in transition metal compounds with the same oxidation state, the Kβ$_{2,5}$ line-shape (including line-width and energy position) depends slightly on the ligand atom. Thus, the increase on the line-width of the Cr-Kβ$_{2,5}$ line in all materials with

Table 2
Kβ line energies after the adsorption processes of trivalent and hexavalent Cr solutions by *P. stratiotes*, *S. auriculata*, activated carbon, and cationic-exchange resin.

Material	Cr ions in solution	Kβ$_{1,3}$ energy[a] (eV)	Kβ$_{2,5}$ energy[a] (eV)	Kβ″ energy[a] (eV)
P. stratiotes	III	5947.47 ± 0.02	5983.87 ± 0.05	5969.14 ± 0.14
	VI	5947.22 ± 0.02	5983.91 ± 0.07	5962.63 ± 0.46
S. auriculata	III	5947.27 ± 0.03	5983.17 ± 0.03	5969.79 ± 0.39
	VI	5947.39 ± 0.02	5985.54 ± 2.56	5962.40 ± 1.44
Activated Carbon	III	5947.08 ± 0.02	5984.09 ± 0.05	5967.71 ± 0.25
	VI	5947.35 ± 0.03	5985.29 ± 0.07	5969.63 ± 0.77
Cationic-exchange resin	III	5947.51 ± 0.03	5985.23 ± 0.10	5963.85 ± 0.12
	VI	5946.54 ± 0.11		

[a] Centroid of Gaussian peak.

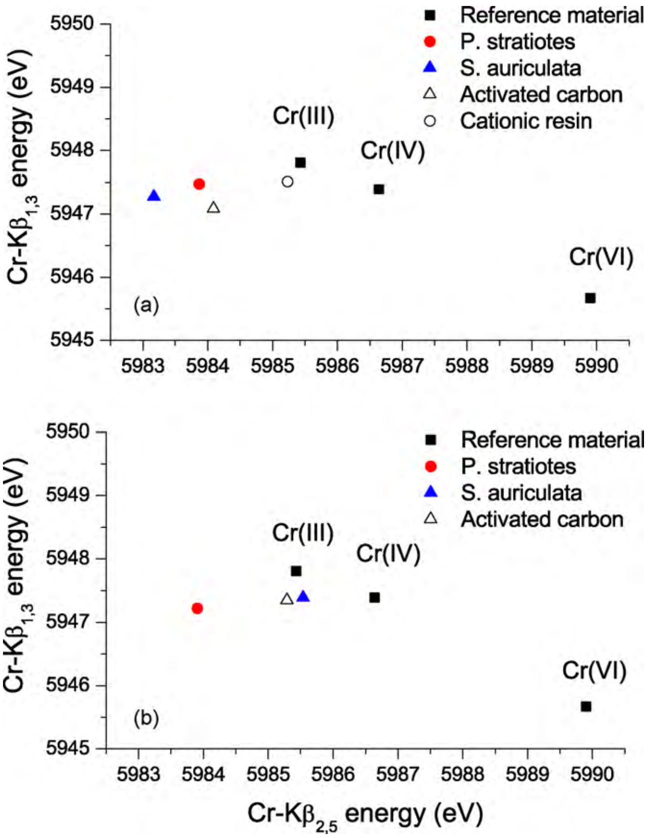

Fig. 7. Comparison between Cr-K$\beta_{2,5}$ energy as function of Cr-K$\beta_{1,3}$ energy of Cr reference materials, *Pistia stratiotes*, *Salvinia auriculata*, activated carbon, and cationic-exchange resin samples after the Cr adsorption processes of (a) trivalent and (b) hexavalent Cr solutions.

respect to Cr reference compounds could be partly explained by the presence of different molecular ligands, which should bind the Cr ions within the complex structure of materials.

On the other hand, in Cr-Kβ spectra of all materials after Cr(VI) adsorption processes (see Figs. 3b, 4b, 5b, and 6b), the peak energies of Cr-K$\beta_{2,5}$ range from 5983.91 to 5985.54 eV (see Table 2), which are nearer to that of Cr(III) reference material (5985.43 ± 0.05 eV, see Table 1) than other ones. In addition, the intensity of Cr-Kβ'' in all spectra, as can be seen in Figs. 3b, 4b, 5b, and 6b, is lower than the intensity of Cr-K$\beta_{2,5}$. In Fig. 7b, the energies of Cr-K$\beta_{1,3}$ and Cr-K$\beta_{2,5}$ lines are closer to that of Cr(III) reference material, suggesting that the Cr(VI) might not be present in all Cr(VI) treated samples, except to the cationic-exchange resin. The low amount of chromium removal (around 7%) by the Cr(VI) treated resin has avoided enhancing the Cr-Kβ satellite lines from the matrix background (see Fig. 6b). Moreover, the Cr-K$\beta_{1,3}$ energy value of 5946.54 ± 0.11 eV belonging to the Cr(VI) treated cationic-exchange resin resembles the peak energy of that for Cr metallic foil (5946.71 ± 0.04 eV), suggesting that the chromium could have been precipitated in low amount in the bulk of resin.

From the previous works using aquatic macrophytes in wetland system (16, 23) the Cr(VI) was reduced to Cr(III) by *P. stratiotes*, *S. auriculata*, and *E. crassipes*, suggesting that the Cr(VI) reduction is mainly due to a physical process. In this way, the present data show that the Cr(VI) reduction to Cr(III) was only observed in Cr uptake experiments using non-living *P. stratiotes*, *S. auriculata*, and activated carbon. However, this kind of behavior was not observed in cationic-exchange resin under the same experimental conditions, as can be seen in Fig. 6a and b, confirming the initial hypothesis that the Cr(VI) reduction to Cr(III) could be mainly associated with an adsorption process, independently of the kind of tested material (dead biomass and activated carbon) for Cr ions removal.

4. Conclusion

The comparison of the high energy region of the Cr-Kβ spectra obtained from Cr(VI) uptake experiments by non-living biomass and activated carbon has shown that there is no evidence of hexavalent oxidation state in all samples, but only a good resemblance with that of Cr(III)-Kβ spectra. The Cr(VI) reduction to Cr(III) was identified to occur in non-living biomass and activated carbon. Experimental data for the cationic-exchange resin have shown a high performance to remove the Cr(III) from an aqueous solution. However, the Cr-Kβ spectra characteristics of Cr(VI) treated cationic-exchange resin samples have revealed that the Cr(VI) was not bound to the surface of it. Independently of the kind of tested material (dead biomass and activated carbon) for Cr ions removal, the adsorption process could be associated with the Cr(VI) reduction.

Acknowledgments

F.R. Espinoza-Quiñones thanks the Brazilian Research Supporting Council (CNPq) for financial support under Project #476724/2007-4. We also thank the Brazilian Light Synchrotron Laboratory (LNLS) for the partial financing of this study (Project #XRD1-8113). A.S.C thanks the Araucaria Research Supporting Agency for awarding the scholarship.

References

[1] M.A. Maine, N.L. Suñe, S.C. Lagger, Chromium bioaccumulation: comparison of the capacity of two floating aquatic macrophytes, Water Res. 38 (6) (2004) 1494–1501.

[2] M.X. Loukidou, A.I. Zouboulis, T.D. Karapantsios, K.A. Matis, Equilibrium and kinetic modeling of chromium (VI) biosorption by *Aeromonas caviae*, Colloids Surf. A: Physicochem. Eng. Aspects 242 (1–3) (2004) 93–104.

[3] X.S. Wang, Y.P. Tang, S.R. Tao, Kinetics, equilibrium and thermodynamic study on removal of Cr(VI) from aqueous solutions using low-cost adsorbent Alligator weed, Chem. Eng. J. 148 (2–3) (2009) 217–225.

[4] J. Acharya, J.N. Sahu, B.K. Sahoo, C.R. Mohanty, B.C. Meikap, Removal of chromium(VI) from wastewater by activated carbon developed from Tamarind wood activated with zinc chloride, Chem. Eng. J. 150 (1) (2009) 25–39.

[5] S. Gupta, B.V. Babu, Removal of toxic metal Cr(VI) from aqueous solutions using sawdust as adsorbent: equilibrium, kinetics and regeneration studies, Chem. Eng. J. 150 (2–3) (2009) 352–365.

[6] S.S. Baral, S.N. Das, P. Rath, Hexavalent chromium removal from aqueous solution by adsorption on treated sawdust, Biochem. Eng. J. 31 (3) (2006) 216–222.

[7] T.N.C. Dantas, A.A. Dantas Neto, M.C.P.A. Moura, E.L. Barros Neto, E.P. Telêmaco, Chromium adsorption by chitosan impregnated with microemulsion, Langmuir 17 (14) (2001) 4256–4260.

[8] F. Gode, E. Pehlivan, A comparative study of two chelating ion-exchange resins for the removal of chromium (III) from aqueous solution, J. Hazard. Mater. 100 (1–3) (2003) 231–243.

[9] T. Shi, Z. Wang, Y. Liu, S. Jia, D. Changming, Removal of hexavalent chromium from aqueous solutions by D301, D314 and D354 anion-exchange resins, J. Hazard. Mater. 161 (2–3) (2009) 900–906.

[10] M.G. Fonseca, M.M. Oliveira, L.N.H. Arakaki, Removal of cadmium, zinc, manganese and chromium cations from aqueous solution by a clay mineral, J. Hazard. Mater. 137 (1) (2006) 288–292.

[11] Y. Lan, C. Li, J. Mao, J. Sun, Influence of clay minerals on the reduction of Cr^{6+} by citric acid, Chemosphere 71 (4) (2008) 781–787.

[12] J.M.T.A. Pietrobelli, A.N. Módenes, M.R. Fagundes-Klen, F.R. Espinoza-Quiñones, Cadmium, copper and zinc biosorption study by non-living *Egeria densa* biomass, Water Air Soil Pollut. 202 (1–4) (2009) 385–392.

[13] A.N. Módenes, J.M.T.A. Pietrobelli, F.R. Espinoza-Quiñones, Cadmium biosorption by non-living aquatic macrophytes *Egeria densa*, Water Sci. Technol. 60 (2) (2009) 293–300.

[14] C. Mahamadi, T. Nharingo, Competitive adsorption of Pb^{2+}, Cd^{2+} and Zn^{2+} ions onto *Eichhornia crassipes* in binary and ternary systems, Bioresour. Technol. 101 (3) (2010) 859–864.

[15] V. Dushenkov, P.B.A.N. Kumar, H. Motto, I. Raskin, Rhizofiltration: the use of plants to remove heavy metals from aqueous streams, Environ. Sci. Technol. 29 (5) (1995) 1239–1245.

[16] C.M. Lytle, F.W. Lytle, N. Yang, J.H. Qian, D. Hansen, A. Zayed, N. Terry, Reduction of Cr(VI) to Cr(III) by wetland plants: potential for in situ heavy metal detoxification, Environ. Sci. Technol. 32 (20) (1998) 3087–3093.

[17] F.R. Espinoza-Quiñones, E.A. Silva, M.A. Rizzutto, S.M. Palácio, A.N. Módenes, N. Szymanski, N. Martin, A.D. Kroumov, Chromium ions phyto-accumulation by three floating aquatic macrophytes from a nutrient medium, World J. Microbiol. Biotechnol. 24 (12) (2008) 3063–3070.

[18] F.R. Espinoza-Quiñones, A.N. Módenes, I.L. Costa Jr., S.M. Palácio, N. Szymanski, D.E.G. Trigueros, A.D. Kroumov, E.A. Silva, Kinetics of lead bioaccumulation from a hydroponic medium by aquatic macrophytes *Pistia stratiotes*, Water Air Soil Pollut. 203 (1–4) (2009) 29–37.

[19] F.R. Espinoza-Quiñones, A.N. Módenes, L.P. Thomé, S.M. Palácio, D.E.G. Trigueros, A.P. Oliveira, N. Szymanski, Study of the bioaccumulation kinetic of lead by living aquatic macrophyte *Salvinia auriculata*, Chem. Eng. J. 150 (2–3) (2009) 316–322.

[20] P. Glatzel, U. Bergmann, High resolution 1s core hole X-ray spectroscopy in 3d transition metal complexes-electronic and structural information, Coord. Chem. Rev. 249 (1–2) (2005) 65–95.

[21] Z. Szafran, R.M. Pike, M.M. Singh, Microscale Inorganic Chemistry. A Comprehensive Laboratory Experience, John Wiley & Sons, New York, 1991.

[22] U. Patnaik, J. Muralidhar, Estimation of chromium in ores and beneficiated products: an ultrasonic approach, Talanta 42 (4) (1995) 553–556.

[23] F.R. Espinoza-Quiñones, N. Martin, G. Stutz, G. Tirao, S.M. Palácio, M.A. Rizzutto, A.N. Módenes, F.G. Silva Jr., N. Szymanski, A.D. Kroumov, Root uptake and reduction of hexavalent chromium by aquatic macrophytes as assessed by high-resolution X-ray emission, Water Res. 43 (17) (2009) 4159–4166.

[24] J.A. Bearden, X-ray wavelengths, Rev. Mod. Phys. 39 (1967) 78–124.

[25] U. Bergmann, C.R. Horne, T.J. Collins, J.M. Workman, S.P. Cramer, Chemical dependence of interatomic X-ray transition energies and intensities–a study of Mn $K\beta''$ and $K\beta_{2,5}$ spectra, Chem. Phys. Lett. 302 (1–2) (1999) 119–124.

[26] M. Torres Deluigi, G. Tirao, G. Stutz, C. Cusatis, J.A. Riveros, Dependence with the oxidation state of x-ray transition energies, intensities and natural line-widths of Cr-Kb spectra, Chem. Phys. 325 (2–3) (2006) 477–484.

[27] V.A. Safonov, L.N. Vykhodtseva, Y.M. Polukarov, O.V. Safonova, G. Smolentsev, M. Sikora, S.G. Eeckhout, P. Glatzel, Valence-to-core X-ray emission spectroscopy identification of carbide compounds in nanocrystalline Cr coatings deposited from Cr(III) electrolytes containing organic substances, J. Phys. Chem. B 110 (46) (2006) 23192–23196.